ELSEVIER

Journal of Alloys and Compounds 223 (1995) 101–110

Journal of ALLOYS AND COMPOUNDS

Neutron diffraction study of the ferromagnetic to antiferromagnetic transition in $La_{0.3}Y_{0.7}Mn_2Ge_2$: phenomenological description of the magnetic behaviour of Mn in $ThCr_2Si_2$ silicides and germanides

G. Venturini [a,*], R. Welter [a], E. Ressouche [b], B. Malaman [a]

[a] *Laboratoire de Chimie du Solide Minéral, Université Henri Poincaré - Nancy I, associé au CNRS (URA 158), B.P. 239, 54506 Vandoeuvre les Nancy Cedex, France*

[b] *CEA/Département de Recherche Fondamentale sur la Matière Condensée/SPSMS-MDN, 1è rue des Martyrs, Grenoble Cedex 9, France*

Received 24 October 1994

Abstract

The magnetic structures of $La_{0.3}Y_{0.7}Mn_2Ge_2$ were determinated by powder neutron study and the magnetic structure of YMn_2Ge_2 was reinvestigated. $La_{0.3}Y_{0.7}Mn_2Ge_2$ is a ferromagnetic compound above about 150 K and an antiferromagnetic compound at lower temperature. The magnetic structure in the ferromagnetic state is canted. At 200 K the Mn moments exhibit a ferromagnetic component ($\mu_{MnF}=1.52(14)$ μ_B) together with an antiferromagnetic component ($\mu_{MnAF}=1.75(9)$ μ_B) within the (001) Mn layers. The ferromagnetic component is ferromagnetically coupled to the ferromagnetic components of the adjacent planes and the antiferromagnetic component leads to a commensurate arrangement (I-centered mode). At 2 K, both components persist and the magnetic structure is a double-cone type. The ferromagnetic component ($\mu_{MnF}=2.10(16)$ μ_B) is antiferromagnetically coupled to the adjacent planes whereas the antiferromagnetic component ($\mu_{MnAF}=1.42(17)$ μ_B) gives rise to an incommensurate arrangement (helical type). In the whole temperature range, the ferromagnetic component is aligned along the *c* axis and the antiferromagnetic component lies in the *a–b* plane. The total Mn moment at 2 K is $\mu_{Mn}=2.54(16)$ μ_B. A Mössbauer study of a ^{57}Fe doped sample indicates that the manganese moments are still ordered above the Curie point. The magnetic structure of YMn_2Ge_2 is a collinear antiferromagnet. The (001) Mn planes are purely ferromagnetic. The Mn moment at 2 K is $\mu_{Mn}=2.23(14)$ μ_B. These results are discussed and it is suggested that the properties of $La_{0.3}Y_{0.7}Mn_2Ge_2$ might account for the magnetic behaviour of $SmMn_2Ge_2$ above the ordering point of the Sm moments. A phenomenological description of the magnetic behaviour of the Mn moment within the RMn_2Si_2 and RMn_2Ge_2 series (R is alkaline earth, rare earth and actinides) is developed.

Keywords: Neutron diffraction; Magnetic behaviour; Manganese

1. Introduction

During the last decade, many works have been devoted to the interesting magnetic properties of the $ThCr_2Si_2$-type structure RMn_2Ge_2 and RMn_2Si_2 compounds (for a review see [1]). Their magnetic structures were described as ferromagnetic Mn (001) planes, ferromagnetically or antiferromagnetically coupled. According to Szytula and Siek [2], the sign of the interplane exchange interaction is sensitive to the in-plane Mn–Mn spacing. These authors have noted that there is a critical distance $d_{Mn-Mn}=2.86$ Å where the magnetic properties change drastically. When the intralayer Mn–Mn spacing is greater than 2.86 Å, the interplane coupling is ferromagnetic whereas it is antiferromagnetic when the spacing is shorter than 2.86 Å. Several compounds such as the ternary $SmMn_2Ge_2$ germanide [3] or the solid solution $La_{1-x}Y_xMn_2Ge_2$ [4] exhibit a temperature dependent ferromagnetic to antiferromagnetic (F–AF) transition related to the thermal contraction of the interatomic distances.

Our own work on the CeFeSi-type structure RMnSi compounds (R ≡ La–Sm, Gd, Tb) [5,6] has shown another particular feature. In these compounds, struc-

* Corresponding author.

SSDI 0925-8388(94)01496-5

turally related to $RMn_2Si(Ge)_2$, there is a correlation between the Mn–Mn interatomic distances and in-plane Mn–Mn coupling. The magnetic structures of the RMnSi compounds (R ≡ La–Nd) consist of antiferromagnetic Mn (001) planes when the Mn–Mn distance is greater than 2.901 Å, whereas the magnetic structure of the TbMnSi compound, where $d_{Mn-Mn} = 2.833$ Å, consists of ferromagnetic Mn layers.

More recent neutron diffraction studies of the ferromagnetic $LaMn_2Si_2$ silicide and RMn_2Ge_2 germanides [7,8] have shown that these $ThCr_2Si_2$ type compounds follow the same trends. In these compounds the ferromagnetic-like behaviour is characterized by large Mn–Mn distances and a part of the Mn moments is quenched into an antiferromagnetic component within the (001) Mn layers. As the known corresponding antiferromagnetic compounds characterized by smaller Mn–Mn distances do not exhibit the same feature, it seems that both phenomena, the occurrence of an antiferromagnetic component together with ferromagnetic behaviour, might be correlated.

In order to check this assumption, we decided to undertake a neutron diffraction study on a sample exhibiting the temperature dependent F–AF transition. Since Sm metal has a too large neutron absorption coefficient, we decided to study a solid solution exhibiting the same phenomenon: the $La_{1-x}Y_xMn_2Ge_2$ solid solution which has been studied by Fujii et al. [4]. These authors have shown that an F–AF transition takes place in the composition range $x = 0.25$–0.35. Later, Kaneko et al. [9] studied extensively the $La_{0.3}Y_{0.7}Mn_2Ge_2$ composition. It is interesting therefore to study this composition using neutron diffraction. Moreover, in such a solid solution of non-magnetic rare earth elements only one magnetic carrier has to be taken into account.

In addition, we reinvestigated the magnetic structure of YMn_2Ge_2, the lower limit of the solid solution, since the corresponding value of the Mn moment ($\mu_{Mn} = 2.85$ μ_B) [10] exhibits some discrepancies within the RMn_2Ge_2 series.

2. Experimental procedures

The compounds were prepared from commercially available high purity elements. Pellets of stoichiometric amounts of the elements were melted in an induction furnace with the cold crucible apparatus. The samples were ground and melted again several times to give better homogenization and then annealed for 2 weeks at 1273 K. The purity of the samples was checked by powder X-ray diffraction technique (Guinier Cu Kα).

The magnetic measurements were carried out on a Faraday balance (above 300 K) and on a MANICS magneto-susceptometer (between 4.2 and 300 K), in fields up to 1.5 T.

Neutron experiments were carried out at the CEN Grenoble. The diffraction patterns were recorded with the one-dimension curved multidetector DN5 at a wavelength $\lambda = 2.4970$ Å. In order to correct for texture effects, following a procedure described in [11], during the refinements we used a fitted coefficient f_{cor} which reflects the importance of preferential orientation.

Using the scattering lengths $b_{Ge} = 8.185$ fm, $b_{Mn} = -3.73$ fm, $b_{La} = 8.24$ fm, $b_Y = 7.75$ fm and the form factor of Mn from [12], the scaling factor, the z_{Ge} atomic positions, f_{cor} and the Mn magnetic moment were refined by the MiXeD crystallographic executive for diffraction (MXD) least-squares-fitting procedure [13].

3. Magnetic measurements

The magnetic properties of $La_{0.3}Y_{0.7}Mn_2Ge_2$ have been extensively studied by Kaneko et al. [9]. Magnetization measurements were taken in order to verify the occurrence of the F–AF transition and to check the width of this transition. Fig. 1 shows the thermal variation of the magnetization and reveals the large width of the magnetic transition. The difference between the magnetic transition temperature of Kaneko et al. [9] and our results is due probably to slight deviation of the composition.

4. Neutron diffraction studies

4.1. $La_{0.3}Y_{0.7}Mn_2Ge_2$

The neutron diffraction patterns at 2 and 200 K are presented in Fig. 2 and the thermal variation of several

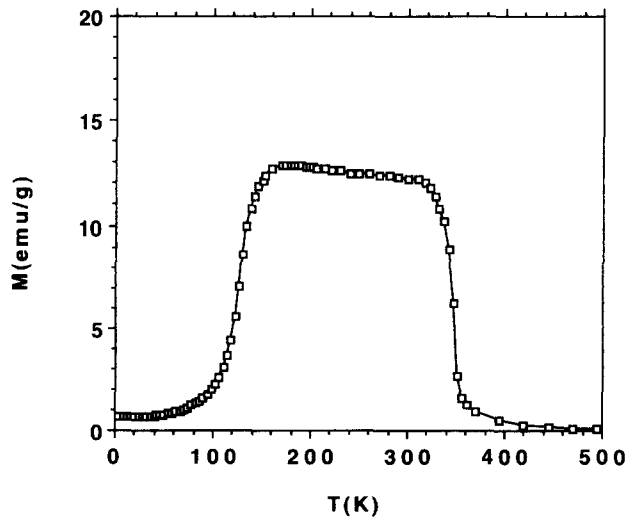

Fig. 1. $La_{0.3}Y_{0.7}Mn_2Ge_2$: thermal variation of the magnetization ($H_{app} = 1$ kOe).

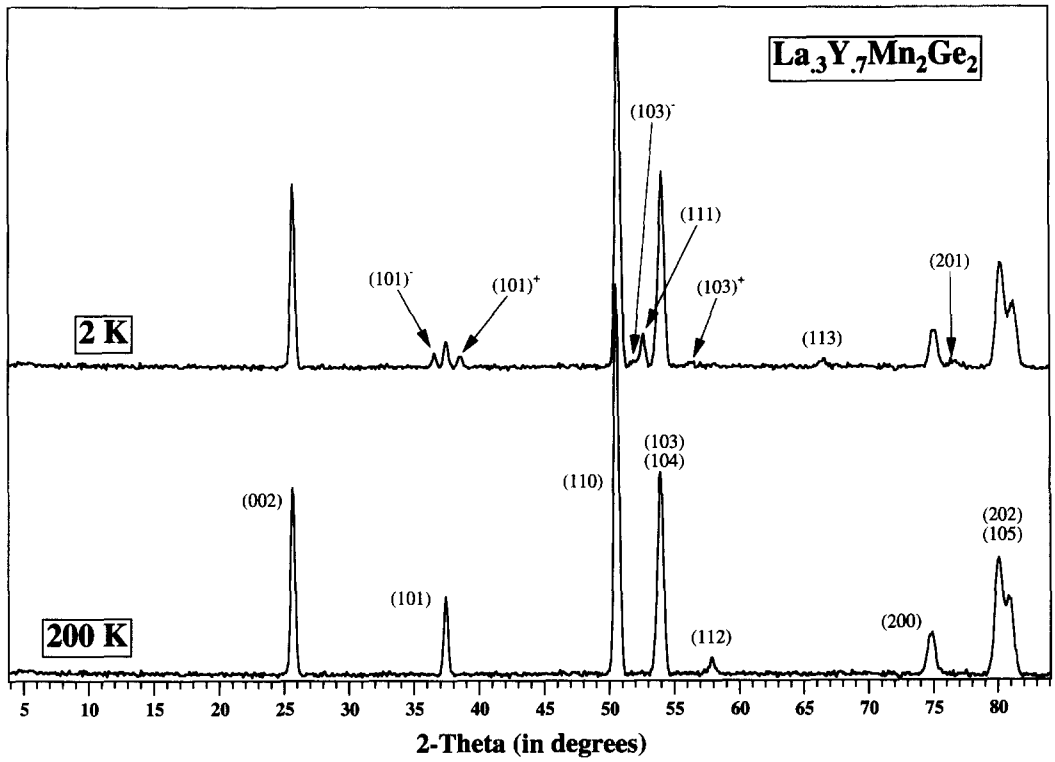

Fig. 2. $La_{0.3}Y_{0.7}Mn_2Ge_2$: neutron diffraction patterns at 2 and 200 K.

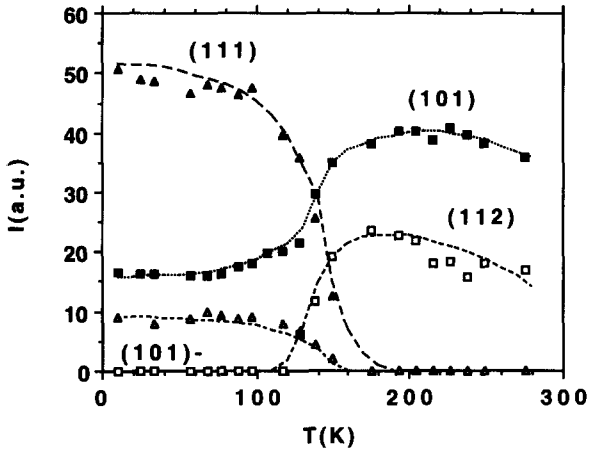

Fig. 3. $La_{0.3}Y_{0.7}Mn_2Ge_2$: thermal variation of some characteristic neutron diffraction lines.

characteristic lines in Fig. 3. Owing to the crystallographic position of the Mn atoms building a C-centred sublattice, the *hkl* lines where $h+k=2n$ are characteristic of ferromagnetic Mn planes. Thus, the C-centred and I-centred (112) line corresponds to the ferromagnetic coupling of ferromagnetic Mn (001) layers. Its intensity is negligible at low temperatures according to the almost zero net value of the nuclear contribution. This line begins to increase around 120 K and accounts well for the appearance of ferromagnetism at this temperature. Above 180 K it decreases slowly following the thermal evolution of the ordered moment. The C-centred and anti I-centred (111) line is characteristic of an antiferromagnetic coupling of ferromagnetic Mn layers. Its value is large at low temperatures when the compound is antiferromagnetic, it begins to decrease strongly around 120 K and has a zero net value around 180 K. The thermal variation of both lines accounts well for the macroscopic magnetic behaviour. The intensity of the anti C-centred (101) line is considerably larger than the nuclear contribution. It reveals the occurrence of an antiferromagnetic component within the (001) Mn layers, as observed previously in the other ferromagnetic RMn_2Ge_2 compounds [7,8]. The intensity of this line decreases strongly at the F–AF transition and, simultaneously, additional lines appear. These lines are indexed as satellites of the *hkl* lines ($h+k=2n+1$) with the wavevector $(0,0,q_z)$. The occurrence of these satellites can be taken as evidence that the in-plane antiferromagnetic component persists through the F–AF transition. Table 1 gives the observed and calculated intensities and the corresponding refined parameters at 2 and 200 K. The magnetic structures are shown in Fig. 4. The high-temperature ferromagnetic structure is canted, the ferromagnetic component is aligned along the *c* axis and the antiferromagnetic component lies in the (001) plane. At low temperature, a double-cone antiferromagnetic structure appears. The thermal variation of the moments is given in Fig. 5. It suggests that the antiferromagnetic component should still be ordered above the Curie point.

Table 1
Calculated and observed intensities, lattice constants and adjustable parameters in $La_{0.3}Y_{0.7}Mn_2Ge_2$ at 200 and 2 K

hkl	200 K		2 K	
	I_c	I_o	I_c	I_o
002	48.0	49.8(7)	47.7	48.5(7)
101	0	–	8.3	8.0(6)
101	39.4	40.1(8)	12.7	16.4(5)
101^+	0	–	8.7	8.5(7)
110	377	385(4)	361	357(4)
111	0	–	46	48(2)
103^-	0	–	8	10(1)
103		–		
004	261	249(4)	254	250(4)
103^+	0	–	9	12(1)
112	22	22(1)	3	–
113	0	–	22	21(2)
200	109	133(4)	100	130(3)
201	0	–	31	21(3)
114	7	–	0	–
202				
105	593	569(5)	539	525(5)
a	4.0604(8)		4.047(2)	
c	10.884(3)		10.864(6)	
z_{Ge}	0.385(1)		0.383(1)	
r_{cor}	1.03(1)		1.02(2)	
μ_{MnF} (μ_B)	1.52(14)		2.10(16)	
μ_{MnAF} (μ_B)	1.75(9)		1.42(17)	
μ_{Mn} (μ_B)	2.31(12)		2.54(16)	
R (%)	5.0		5.1	

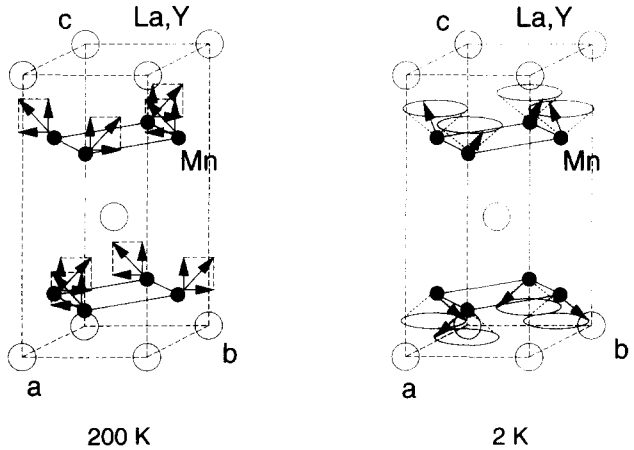

Fig. 4. Magnetic structures of $La_{0.3}Y_{0.7}Mn_2Ge_2$ at 2 and 200 K.

4.2. YMn_2Ge_2

The magnetic structure of YMn_2Ge_2 was refined at 2 and 300 K. The calculated and observed intensities and the corresponding refined parameters are given in Table 2. The Mn moment at 2 K (2.23 μ_B) is in good accordance with the value measured in $DyMn_2Ge_2$ (2.3(1) μ_B) by single-crystal neutron diffraction [14]. Moreover this refinement clearly shows that there is no magnetic contribution on the (101) line: the Mn layers are purely ferromagnetic.

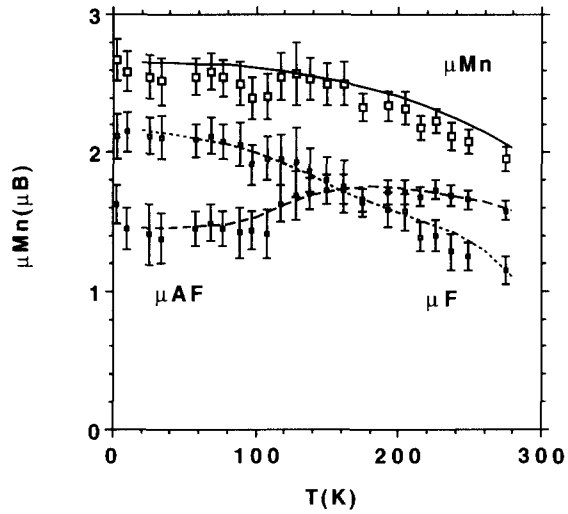

Fig. 5. $La_{0.3}Y_{0.7}Mn_2Ge_2$: thermal variation of the total Mn moment and of its ferromagnetic and antiferromagnetic components.

Table 2
Calculated and observed intensities, lattice constants and adjustable parameters in YMn_2Ge_2 at 300 and 2 K

hkl	300 K		2 K	
	I_c	I_o	I_c	I_o
002	44.2	45.3(5)	44.0	43.9(5)
101	13.3	13.9(6)	13.6	14.0(6)
110	357.4	361(2)	322.5	318(2)
111	39.5	40(2)	46.0	45(2)
004	39.6	34(2)	33.8	46(2)
103	209.1	207(2)	166.1	164(2)
112	2.1	–	4.3	–
113	18.6	17(2)	21.6	19(2)
200	98.5	98(2)	88.9	107(3)
114				
201	23.8	25(2)	27.2	36(3)
105	299.3	276(9)	296.1	293(4)
202	193.3	165(5)	193.1	199(4)
a	3.994(2)		3.982(2)	
c	10.861(6)		10.848(6)	
z_{Ge}	0.382(1)		0.386(1)	
r_{cor}	1.03(1)		1.03(1)	
μ_{Mn} (μ_B)	1.96(11)		2.23(14)	
R (%)	6.9		4.9	

5. Mössbauer spectroscopy

Following a procedure undertaken by Nowik et al. on ^{57}Fe doped RMn_2Ge_2 compounds [15], several spectra of $La_{0.3}Y_{0.7}Mn_{1.9}Fe_{0.1}Ge_2$ were recorded at 300, 370 and 410 K. The hyperfine parameters are gathered in Table 3. The main information derived from these preliminary results is the occurrence of a non-zero

Table 3
Hyperfine parameters of the ^{57}Fe doped sample $La_{0.3}Y_{0.7}Mn_{1.9}Fe_{0.1}Ge_2$ at 410, 370 and 300 K

T (K)	Γ (mm s^{-1})	IS (mm s^{-1})	EQ (mm s^{-1})	H (kOe)	P (%)
410	0.32	0.17	0.145	0	100
370	0.31	0.13	0.244	27.6	80
	0.31	0.25	0.113	10.4	20
300	0.33	0.27	−0.045	100.4	82
	0.21	0.27	−0.070	89.6	18

hyperfine field at 370 K, above the Curie point, and the relative values of the effective quadrupole interaction which have a weak negative value at 300 K and a large positive value at 370 K.

The occurrence of a non-zero hyperfine field at 370 K indicates that the compound is still magnetically ordered above the Curie point, as suggested by the thermal variation of the in-plane antiferromagnetic component. This result is in fair accordance with the data of Nowik et al. for the ternary RMn_2Ge_2 compounds [15].

The change in sign of the effective quadrupole interaction indicates a change in magnetic hyperfine field direction, i.e. a reorientation of the Mn moments. The value of both Mn moment components at 300 K determinated by neutron diffraction leads to a moment direction at about 60° from the c axis. According to the Mössbauer results, the moment direction at 370 K should be the c axis, as observed previously in $CaMn_2Ge_2$ [16].

6. Discussion

6.1. Evolution of the Mn magnetic behaviour in the $La_{1-x}Y_xMn_2Ge_2$ solid solution

The neutron diffraction study of $La_{1-x}Y_xMn_2Ge_2$ provides new information about the F–AF transition observed by magnetometric measurements in several $ThCr_2Si_2$-type silicides and germanides such as $SmMn_2Ge_2$ [3], $La_{1-x}Y_xMn_2Ge_2$ [4], $La_{1-x}Y_xMn_2Si_2$ [17], $Ce_{1-x}La_xMn_2Si_2$ [18], $CeMn_2Si_{2-x}Ge_x$ [19].

Two main phenomena take place at the magnetic transition. The interplane coupling of the ferromagnetic component within the (001) Mn layer changes from ferromagnetic at high temperature to antiferromagnetic at lower temperature. The interplane coupling of the antiferromagnetic component changes from a commensurate arrangement of the moment components to an incommensurate arrangement. Before this work, we assumed that the antiferromagnetic component might disappear at the F–AF magnetic transition. This assumption is refuted by the occurrence of the (101) satellites in the low temperature spectra. Nevertheless, the thermal evolution of the moment shows discontinuities of the ferromagnetic and antiferromagnetic components at the transition (Fig. 5). The ferromagnetic component increases slightly when the temperature decreases, while the antiferromagnetic component decreases in the same time. The ferromagnetic component in the ferromagnetic state is close to 1.5 μ_B as in the ferromagnetic RMn_2Ge_2 (R ≡ La–Nd) and $LaMn_2Si_2$ compounds [7,8]. The ferromagnetic component in the antiferromagnetic state is larger (2.2 μ_B) and close to the values measured in the antiferromagnetic RMn_2Ge_2 (R ≡ Tb–Er) and RMn_2Si_2 (R ≡ Ce–Nd, Tb–Er) compounds [14,20–25]. At the transition, the total Mn moment does not show any significant discontinuity. All these phenomena probably account well for the magnetic behaviour of the intensively studied $SmMn_2Ge_2$ compound [3], at least above the ordering point of the Sm moments. The numerous results obtained on the physical properties of this compound could be re-examined in the light of this new information.

The thermal variation of the cell parameters plotted in Fig. 6 exhibits the same feature as the published values of Kaneko et al. [9] although the width of the transition is broader. The a parameter decreases strongly at the F–AF transition whereas the c parameter increases slightly. The value of the Mn–Mn spacing (d_{Mn-Mn} = 2.864(2) Å) in the antiferromagnetic state is close to the critical value proposed by Szytula and Siek [2].

The thermal variation of the q_z component of the wavevector is presented in Fig. 7 together with the values measured in the other RMn_2Ge_2 (R = La, Pr, Nd) and $LaMn_2Si_2$ compounds [7,8]. It shows a continuous decrease of the transition temperature and of the q_z value with the cell volume.

The $La_{0.3}Y_{0.7}Mn_2Ge_2$ compound exhibits all the main magnetic features encountered in the RMn_2Ge_2 and RMn_2Si_2 silicides and germanides. For comparison, the

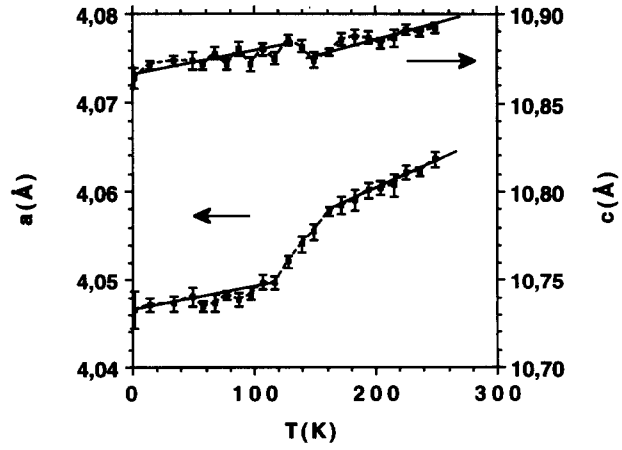

Fig. 6. $La_{0.3}Y_{0.7}Mn_2Ge_2$: thermal variation of the cell parameters.

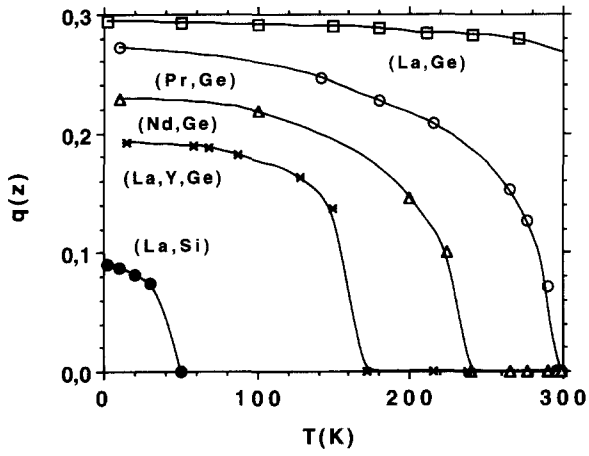

Fig. 7. Thermal variation of the q_z component of the wavevector in RMn_2Ge_2 (R ≡ La, Pr, Nd, (La, Y)) and $LaMn_2Si_2$ compounds.

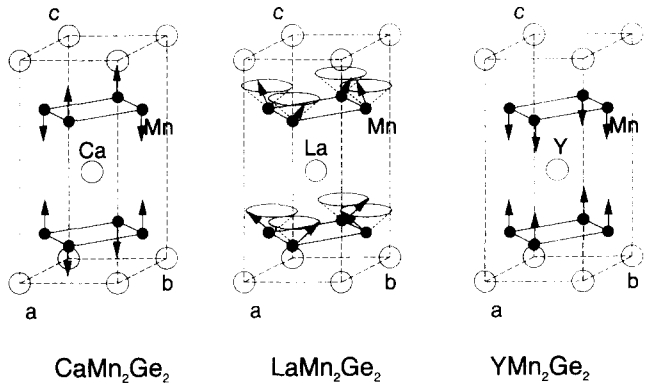

Fig. 8. Magnetic structures of $CaMn_2Ge_2$, $LaMn_2Ge_2$ and YMn_2Ge_2 at 2 K.

magnetic structures of $CaMn_2Ge_2$ [16], $LaMn_2Ge_2$ [7] and YMn_2Ge_2 are presented in Fig. 8.

Within the studied temperature range, both ferromagnetic and antiferromagnetic components occur within the (001) Mn layers. Moreover, from Mössbauer experiments it can be derived that a purely antiferromagnetic plane occurs above the Curie point.

The interplane coupling of the ferromagnetic component is temperature dependent, as in $SmMn_2Ge_2$, and yields the F–AF transition.

The interplane coupling of the antiferromagnetic components leads either to a commensurate arrangement, as observed previously in the RMn_2Ge_2 compounds (R ≡ Ca, Ba, Pr, Nd), or to an incommensurate arrangement as observed in the RMn_2Ge_2 compounds (R ≡ La, Ce) and in RMn_2Ge_2 (R ≡ Pr, Nd) at low temperatures [7,8,16].

6.2. Phenomenological description of the magnetic behaviour of Mn in the $ThCr_2Si_2$ type structure compounds

The behaviour of $La_{0.3}Y_{0.7}Mn_2Ge_2$ is a summary of the magnetic properties encountered in the RMn_2Si_2 and RMn_2Ge_2 compounds. It allows us to give a phenomenological description of these magnetic properties.

Three main phenomena have to be described.

(1) The in-plane magnetic coupling which may be purely ferromagnetic, purely antiferromagnetic or mixed.

(2) The interplane coupling of the ferromagnetic component which may be ferromagnetic or antiferromagnetic. Up to now, most works on the RMn_2Ge_2 and RMn_2Si_2 compounds have been devoted to this phenomenon and the in-plane Mn–Mn spacing criterion is the main result of these studies [2].

(3) The interplane coupling of the antiferromagnetic component which leads to a commensurate arrangement or to an incommensurate arrangement.

6.2.1. In-plane magnetic coupling

Up to now, it was generally assumed that the Mn (001) planes in the $ThCr_2Si_2$ compounds were purely ferromagnetic. Our studies of the RMn_2Ge_2 compounds (R ≡ Ca, Ba, La–Nd) have shown that the magnetic behaviour of these layers is more complicated [7,8,16]. All the known results for the RMn_2Ge_2 and RMn_2Si_2 magnetic structures (R is alkaline earth, rare earth and actinides) allow us to define a distance-dependent criterion, as done previously with the interplane couplings. When the in-plane Mn–Mn distance is shorter than about 2.86 Å, the Mn layers are purely ferromagnetic; when the Mn–Mn distance is longer than about 2.86 Å, the occurrence of at least an antiferromagnetic component has been demonstrated. In the RMn_2Si_2 series the upper limit of the Mn–Mn distance associated with ferromagnetic couplings is found in $PrMn_2Si_2$ (d_{Mn-Mn} = 2.847 Å) [24] and the lower limit of the Mn–Mn distance associated with mixed planes is found in $LaMn_2Si_2$ (d_{Mn-Mn} = 2.907 Å) [7]. In the RMn_2Ge_2 series the upper limit of the Mn–Mn distance associated with ferromagnetic couplings is found in $TbMn_2Ge_2$ (d_{Mn-Mn} = 2.832 Å) [22] and the lower limit of the Mn–Mn distance associated with mixed planes is found in $La_{0.3}Y_{0.7}Mn_2Ge_2$ (d_{Mn-Mn} = 2.864 Å). The alkaline earth and actinide compounds do not exhibit large deviations from this scheme. The occurrence of ferromagnetic Mn planes has been demonstrated in $ThMn_2Ge_2$ [26]. The Mn–Mn spacing (d_{Mn-Mn} = 2.880 Å) is the largest found in an actinide $ThCr_2Si_2$-type structure compound. The occurrence of antiferromagnetic planes is demonstrated in $CaMn_2Ge_2$ [16]. The Mn–Mn spacing (d_{Mn-Mn} = 2.931 Å) is the shortest found in an alkaline earth $ThCr_2Si_2$-type structure compound. From this review, it obviously appears that Mn–Mn spacings shorter than about 2.86 Å lead to ferromagnetic Mn planes, and Mn–Mn spacings greater than about 2.86 Å lead to antiferromagnetic or mixed Mn planes, whatever the valency of the R element. A summary of these correlations is given in Fig. 9. This

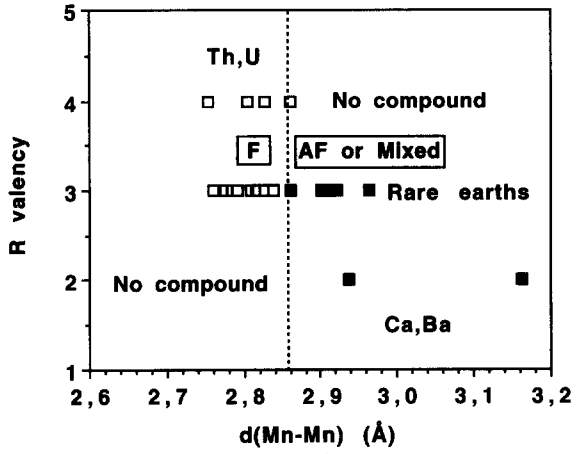

Fig. 9. Schematic representation of the in-plane Mn magnetic couplings in the RMn_2Si_2 and RMn_2Ge_2 compounds as a function of the Mn–Mn separation and R valency.

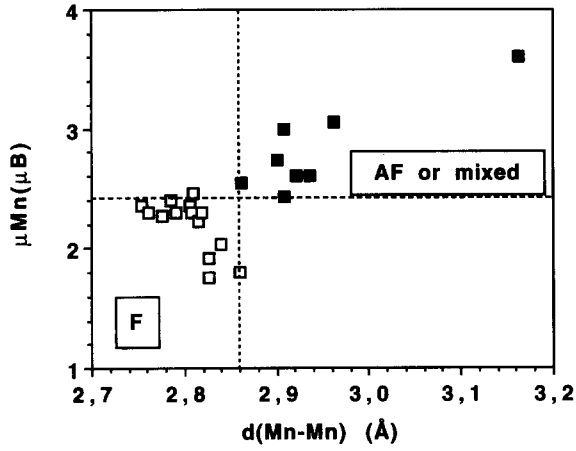

Fig. 10. Schematic representation of the in-plane Mn magnetic couplings in the RMn_2Si_2 and RMn_2Ge_2 compounds as a function of the Mn–Mn separation and magnitude of the Mn moment.

criterion may be extended to the RMnSi compounds which also contain the same Mn square net. In this series, the occurrence of ferromagnetic planes has been demonstrated only for TbMnSi where the Mn–Mn distance is 2.833 Å. The lower limit of the Mn–Mn distance associated with antiferromagnetic planes is found in NdMnSi ($d_{Mn-Mn}=2.901$ Å) [5,6].

A second remark concerns the correlations between the in-plane magnetic coupling and the value of the Mn moment. A plot of the Mn moment as a function of the Mn–Mn separation is given in Fig. 10. The ferromagnetic range is separated from the antiferromagnetic range by the Mn–Mn interatomic distance criterion defined previously but also by a critical value of the Mn moment. Thus, antiferromagnetic Mn planes occur when the Mn moment is greater than about 2.5 μ_B and ferromagnetic planes when the moment is smaller than 2.5 μ_B.

A further remark concerns the occurrence of the mixed planes. The study of $LaMn_2Si_2$ has shown that, above the Curie point, this compound is built of pure antiferromagnetic Mn planes. According to the Mössbauer studies of Nowik et al. on the RMn_2Ge_2 compounds [15] and according to our study on ^{57}Fe doped $La_{0.3}Y_{0.7}Mn_2Ge_2$, the germanides behave similarly. The occurrence of mixed planes could be the result of additional exchange interactions acting only at low temperature so that it may be assumed that isolated Mn planes behave ferromagnetically or antiferromagnetically as a function of the Mn–Mn separation only. Moreover, the appearance of the mixed planes seems to be a critical phenomenon which only occurs in rare earth compounds with $ThCr_2Si_2$-type structure and only at low temperature. Such mixed planes do not occur in the CeFeSi-type compounds or in the alkaline earth $ThCr_2Si_2$-type germanides. Assuming such competing interactions, the ratio of the antiferromagnetic moment to the total moment might be an indirect measure of their relative strengths. This ratio as a function of the Mn–Mn separation is plotted in Fig. 11 for all known diamagnetic R element compounds. Assuming that the strength of the additional interactions does not change for a given R valency, it appears that the ratio decreases when the Mn–Mn separation rises to the critical distance. The particular behaviour of the alkaline earth compounds might be related to weaker additional interactions, in relation with a modification of their electronic structure.

When it is assumed that an internal molecular field is able to align ferromagnetically a component of the Mn moment within the (001) layer, one would expect that an external field would act similarly. Kaneko et al. [9] took high field magnetic measurements on $La_{0.3}Y_{0.7}Mn_2Ge_2$ and did not find any metamagnetic transition up to 150 kOe. The maximum magnetization value at 4.2 K and under 150 kOe is 60 emu g^{-1}, i.e. 1.93 μ_B per Mn close to the value of the ferromagnetic component. In this compound, where the Mn–Mn dis-

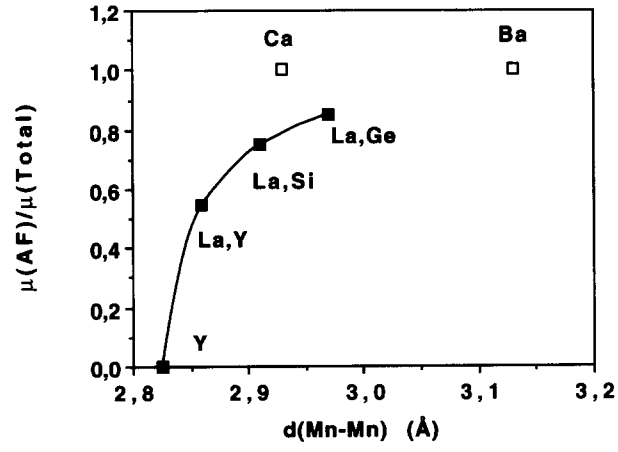

Fig. 11. Variation of the ratio μ_{AF}/μ_{Total} with the interatomic Mn–Mn spacings in the $LaMn_2Si_2$ and RMn_2Ge_2 (R = Ca, Ba, La, (La, Y)) compounds.

tances are close to the critical value, the in-plane antiferromagnetic coupling remains strong.

6.2.2. Interplane coupling of the ferromagnetic component

As previously noted, many works have been devoted to this subject [2,4,17–19]. Within the rare earth silicides and germanides, an Mn–Mn spacing criterion has been elaborated which well fits the observations. For interatomic Mn–Mn distances greater than 2.86 Å, the interplane coupling is ferromagnetic whereas it is antiferromagnetic for Mn–Mn spacings shorter than 2.86 Å. The present study confirms this rule since the interplane coupling changes in the range 2.87–2.86 Å. Nevertheless, there are several examples of the contrary in other R element systems. The alkaline earth $CaMn_2Ge_2$ and $BaMn_2Ge_2$ compounds should be ferromagnetic according to this rule. Nevertheless these compounds do not give evidence of any ferromagnetism [16]. At high temperature, the rare earth compounds behave similarly [7,15]. The actinide compound UMn_2Si_2 is ferromagnetic [27] although the Mn–Mn spacings are shorter than 2.86 Å, and $ThMn_2Si_2$ is antiferromagnetic [26] although the Mn–Mn spacings are greater than in UMn_2Si_2. Study of the solid solution $Th_{1-x}U_xMn_2Si_2$ gives evidence of an AF–F transition as a function of the x value and hence as a function of the Mn–Mn spacing [28]. In this case, Mn–Mn spacings larger than about 2.828 Å yield antiferromagnetic structures and shorter Mn–Mn spacings yield ferromagnetism. A summary of the interplane couplings as a function of the in-plane Mn–Mn separations and of the R valency is given in Fig. 12. These examples show that the interplane coupling is not unambiguously determined by the Mn–Mn spacing alone. The R valency also influences this coupling and the interplane exchange interaction is inverted in the actinide compounds. In the alkaline earth compounds, the interplane interaction is perhaps too weak to act on the Mn antiferromagnetic plane and cannot reverse the antiferromagnetic Mn moments.

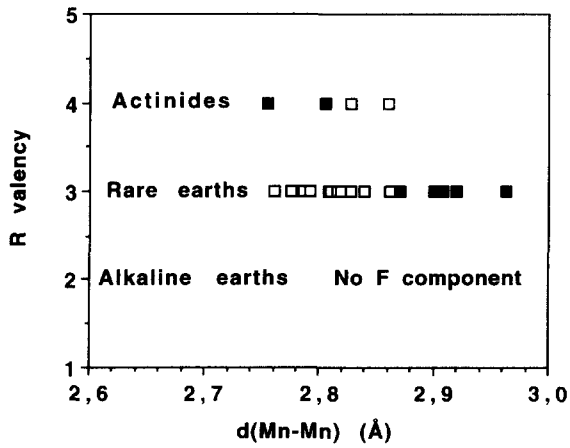

Fig. 12. Schematic representation of the ferromagnetic component interplane couplings in RMn_2Si_2 and RMn_2Ge_2 compounds as a function of the Mn–Mn separation and R valency (■ ferromagnetic, □ antiferromagnetic).

6.2.3. Interplane coupling of the antiferromagnetic component

Two arrangements of the antiferromagnetic component have been encountered within the $ThCr_2Si_2$-type structure compounds. The alkaline earth compounds are always characterized by a commensurate arrangement of these components whereas the Nd and the Pr compounds and $La_{0.3}Y_{0.7}Mn_2Ge_2$ are commensurate only at high temperature [8,16]. The resulting magnetic structure retains the I-centred mode of the chemical cell (Fig. 13). The Mn moments related by the body-centred translation (1–1′) are ferromagnetically coupled, the adjacent Mn moments lying on the same [001] axis (1–2′) are antiferromagnetically coupled.

The Ce and La compounds have incommensurate magnetic structure in the whole temperature range studied. The Nd and the Pr compounds and the $La_{0.3}Y_{0.7}Mn_2Ge_2$ solid solution exhibit an incommensurate magnetic structure only at low temperatures. In this incommensurate arrangement the moments of Mn atoms related by the body-centred translation (1–1′) make an angle going from 0° to about 60° as a function of the value of q_z, the moment of the adjacent Mn atoms (1–2′) making an angle going from 180° to 120°.

The interplane exchange interactions (J_1, J_2) are either mediated by the conduction electron or by super–super exchange via the Mn–X–X–Mn bonds. When the conduction electrons are responsible for these interactions, the oscillatory character of the magnetic interactions depends either on the interatomic spacings ($d_{1-1'}$, $d_{1-2'}$) or on the electronic structure. The difference in electronic structure may account for the differences between the R^{2+} and R^{3+} compounds. The interatomic spacing may account for the differences observed within the

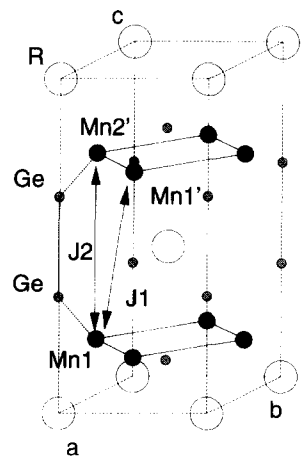

Fig. 13. Representation of the $ThCr_2Si_2$-type structure cell, showing the various Mn–Mn interplane interactions.

series of rare earth compounds. A plot of the maximum value of q_z and of the transition temperature T_t from the commensurate to the incommensurate state vs. the $d_{1-1'}$ distance is given in Fig. 14. It shows the fair correlations between q_z and T_t on the one hand and the interplane spacings on the other hand. When the exchange integrals (J_1, J_2) between a given Mn moment and its two near neighbours in the adjacent planes (see Fig. 13) have the same sign, the antiferromagnetic plane configuration gives rise to a frustrated situation and may stabilize an incommensurate structure. Thus, the value of q_z might be correlated to the relative strengths of the interactions. When the exchange integrals have opposite signs or when one of them dominates the other, a commensurate structure becomes stable.

The commensurate–incommensurate (C–I) transition and the F–AF transition occur simultaneously in $La_{0.3}Y_{0.7}Mn_2Ge_2$. This phenomenon might be related to the sudden increase in the c/a ratio at the F–AF transition and consequently to corresponding variation of the interatomic distances. It is worthwhile to note that in $NdMn_2Ge_2$ and in $PrMn_2Ge_2$ the C–I transition just depends on the temperature since no F–AF transition occurs in these compounds.

At the F–AF transition, the interplane coupling of the ferromagnetic component changes abruptly from ferromagnetic to antiferromagnetic and the magnetic contribution to the I-centred lines (112) is transferred to the anti I-centred lines (111). If the interplane coupling of the antiferromagnetic components were also inverted at the F–AF transition, the magnetic contribution to the (hkl) peaks ($h+k=2n+1$) would be transferred from the I-centred lines (101) to the anti I-centred lines (100) or satellites of these lines. The phenomena occurring in $La_{0.3}Y_{0.7}Mn_2Ge_2$ indicate rather that the sign of the involved exchange integral does not change much and that each component behaves independently.

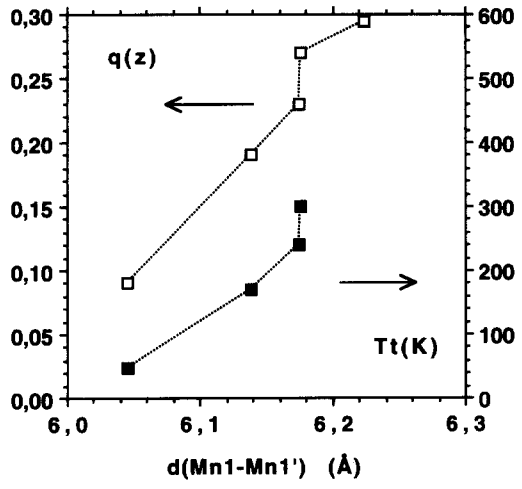

Fig. 14. Variation of the q_z value and of the commensurate–incommensurate transition temperature T_t with the interplane Mn1–Mn1' distance.

7. Conclusions

The neutron diffraction study of the F–AF transition in $La_{0.3}Y_{0.7}Mn_2Ge_2$ has revealed some unexpected results. The transition from the ferromagnetic state to the antiferromagnetic state is not correlated to the vanishing of the antiferromagnetic component within the (001) layers. The magnetic behaviour of the Mn moment in the $ThCr_2Si_2$ compounds may be divided into three contributions. The in-plane magnetic coupling, the interplane coupling of the ferromagnetic component within the (001) plane and the interplane coupling of the antiferromagnetic component. The in-plane magnetic coupling is rather well correlated to the Mn–Mn spacing as well as to the value of Mn moment. The interplane coupling of the ferromagnetic component fits well the previously defined interatomic Mn–Mn distance criterion in the case of the rare earth compounds. This behaviour is significantly different in the case of alkaline earths or actinide compounds. The interplane coupling of the antiferromagnetic component is also temperature dependent but the phenomena involved are not significantly correlated to the F–AF transition. The complex behaviour of the $ThCr_2Si_2$ type structure manganese compounds arises from the interplay between these three main interactions.

References

[1] A. Szytula and J. Leciejewicz, Magnetic properties of ternary intermetallic compounds of the RT_2X_2 type, *Handbook on the Physics and Chemistry of Rare Earths*, Vol. 12, 1989, Chapter 83, p. 133.
[2] A. Szytula and S. Siek, *J. Magn. Magn. Mater., 27* (1982) 49.
[3] H. Fujii, T. Okamoto, T. Shigeoka and N. Iwata, *Solid State Commun., 53* (8) (1985) 715.
[4] H. Fujii, M. Isoda, T. Okamoto, T. Shigeoka and N. Iwata, *J. Magn. Magn. Mater., 54–57* (1986) 1345.
[5] R. Welter, G. Venturini and B. Malaman, *J. Alloys Comp., 206* (1994) 55.
[6] R. Welter, G. Venturini, E. Ressouche and B. Malaman, *J. Alloys Comp., 210* (1994) 273.
[7] G. Venturini, R. Welter, E. Ressouche and B. Malaman, *J. Alloys Comp., 210* (1994) 213.
[8] R. Welter, G. Venturini, E. Ressouche and B. Malaman, *J. Alloys Comp.*, in press.
[9] T. Kaneko, T. Kanomata, H. Yasui, T. Shigeoka, M. Iwata and Y. Nakagawa, *J. Phys. Soc. Jpn., 61* (11) (1992) 4164.
[10] S. Siek, A. Szytula and J. Leciejewicz, *Solid State Commun., 39* (1981) 863.
[11] R. Welter, G. Venturini and B. Malaman, *J. Alloys Comp., 189* (1992) 49.
[12] C. Stassis, H.W. Deckman, B.N. Harman, J.P. Desclaux and A.J. Freeman, *Phys. Rev. B, 15* (1977) 369.
[13] P. Wolfers, *J. Appl. Crystallogr., 23* (1990) 554.

[14] H. Kobayashi, H. Onodera, Y. Yamaguchi and H. Yamamoto, *Phys. Rev. B, 43* (1) (1991) 728.
[15] I. Nowik, Y. Levy, I. Felner and E.R. Bauminger, *J. Magn. Magn. Mater.*, to be published.
[16] B. Malaman, G. Venturini, R. Welter and E. Ressouche, *J. Alloys Comp., 210* (1994) 209.
[17] E.V. Sampathkumaran, R.S. Chaughule, K.V. Gopalakrishnan, S.K. Malik and R. Vijayaraghavan, *J. Less-Common Met., 92* (1983) 35.
[18] A. Szytula and S. Siek, *J. Magn. Magn. Mater., 27* (1982) 49.
[19] P. Hill and N. Ali, *J. Appl. Phys., 73* (10) (1993) 5683.
[20] J. Leciejewicz and A. Szytula, *Solid State Commun., 49* (4) (1984) 361.
[21] J. Leciejewicz, A. Szytula, W. Bazela and S. Siek, *J. Magn. Magn. Mater., 89* (1990) 29.
[22] J. Leciejewicz, S.Siek and A. Szytula, *J. Magn. Magn. Mater., 40* (1984) 265.
[23] S. Siek, A. Szytula and J. Leciejewicz, *Phys. Status Solidi A, 46* (1978) K101.
[24] R. Welter, G. Venturini, D. Fruchart and B. Malaman, *J. Alloys Comp., 191* (1993) 263.
[25] T. Shigeoka, N. Iwata, H. Fujii and T. Okamoto, *J. Magn. Magn. Mater., 54–57* (1986) 1343.
[26] Z. Ban, L. Omejec, A. Szytula and Z. Tomkowicz, *Phys. Status Solidi A, 27* (1975) 333.
[27] A. Szytula, S. Siek, J. Leciejewicz, A. Zygmunt and Z. Ban, *J. Phys. Chem. Solids, 49* (9) (1988) 1113.
[28] W. Bazela and A. Szytula, *J. Magn. Magn. Mater., 82* (1989) 151.